

Nesting Induced Large Magnetoelasticity in the Iron Arsenide Systems

I. Paul

Laboratoire Matériaux et Phénomènes Quantiques,
Université Paris Diderot-Paris 7 & CNRS, UMR 7162, 75205 Paris, France
(Dated: March 12, 2022)

A novel feature of the iron arsenides is the magnetoelastic coupling between the long wavelength in-plane strains of the lattice and the collective spin fluctuations of the electrons near the magnetic ordering wavevectors. Here, we study its microscopic origin from an electronic model with nested Fermi pockets and a nominal interaction. We find the couplings diverge with a power-law as the system is tuned to perfect nesting. Furthermore, the theory reveals how nematicity is boosted by nesting. These results are relevant for other systems with nesting driven density wave transitions.

PACS numbers: 74.70.Xa, 75.80.+q, 71.10.-w, 74.25.Kc

I. INTRODUCTION

A possible source of complexity in correlated metals is the coupling between apparently unrelated degrees of freedom. The richness that can ensue from it is aptly demonstrated by the iron arsenide (FeAs) systems that are being studied intensely for their high temperature superconductivity and for their intricate non-superconducting phases.^{1,2} At low doping they undergo a transition from a tetragonal to orthorhombic crystal structure at temperature T_S (where C_4 symmetry is broken) followed closely by an antiferromagnetic (AF) transition (where time reversal symmetry is broken) at $T_N \leq T_S$. The presence of the two seemingly disparate transitions in close proximity suggests the presence of magnetoelastic coupling (MEC) between their order parameters.³⁻⁸ The purpose of this paper is to study the origin of MEC from a microscopic point of view, and to argue that Fermi surface nesting enhances their magnitudes dramatically. The theory also shows how nesting enhances nematicity, which is yet another intriguing and intensely-studied property of FeAs.

An important band structure feature of these materials, which is well established both theoretically and experimentally, is the nesting between the circular hole pockets centered around $(0,0)$ and the elliptic electron pockets centered at $(\pi,0)$ and $(0,\pi)$ of the Brillouin zone defined by the plane of Fe atoms with 1Fe/cell.⁹⁻¹¹ Its importance further underlined by the fact that the AF order involves a nesting wavevector, either $\mathbf{Q}_1 = (\pi,0)$ or $\mathbf{Q}_2 = (0,\pi)$, implying a nesting driven density wave transition from a paramagnetic metal.¹²

Besides the fact that T_S and T_N track each other closely in the temperature-doping phase diagram, there are few other indirect evidences of MEC in the FeAs systems. (1) *Ab initio* calculations show that the electron-phonon coupling strength in the magnetic state increases by 50% compared to the paramagnetic one.¹³ (2) The magnetic transition temperature T_N is very sensitive to uniaxial pressure.¹⁴⁻¹⁶ (3) Applying uniaxial pressure detwins single crystals in the AF phase.¹⁷ From the theoretical side, the effects of MEC has been studied phenomenologically.^{5,6,15} It has been shown that the cou-

pling plays a central role in establishing a universal phase diagram of the FeAs systems.⁵ In particular, the presence of tricritical points at which the AF transition changes character from first to second order were predicted, and it has later been confirmed experimentally.¹⁸ More recently, an *ab initio* study of the effects of uniaxial pressure has interpreted their results using MEC.¹⁹ However, to the best of our knowledge, until now there has been no investigation of the microscopic origin of the MEC.

II. MODEL

In FeAs the MEC coupling between the magnetostructural order parameters and the associated long wavelength fluctuations can be expressed, using symmetry arguments, by the effective Hamiltonian

$$\begin{aligned} \mathcal{H}_{ME} = \sum_{\mathbf{q}, \mathbf{p}} \Big\{ & \lambda_O(q, p) \left[u_O(\mathbf{q}) \mathbf{M}_{1, \mathbf{q}+\mathbf{p}}^\dagger \cdot \mathbf{M}_{1, \mathbf{p}} - u_O(\mathbf{q}') \right. \\ & \times \mathbf{M}_{2, \mathbf{q}'+\mathbf{p}'}^\dagger \cdot \mathbf{M}_{2, \mathbf{p}'} \Big] + \lambda_A(q, p) \left[u_A(\mathbf{q}) \mathbf{M}_{1, \mathbf{q}+\mathbf{p}}^\dagger \right. \\ & \left. \left. \cdot \mathbf{M}_{1, \mathbf{p}} + u_A(\mathbf{q}') \mathbf{M}_{2, \mathbf{q}'+\mathbf{p}'}^\dagger \cdot \mathbf{M}_{2, \mathbf{p}'} \right] \right\}. \end{aligned} \quad (1)$$

Here $\mathbf{M}_{\alpha, \mathbf{q}} \equiv \mathbf{M}(\mathbf{Q}_\alpha + \mathbf{q})$ with $\alpha = (1, 2)$ denote the magnetization around the ordering wavevectors, $u_O(\mathbf{q})$ and $u_A(\mathbf{q})$ are the Fourier transforms of the orthorhombic distortion $u_O(\mathbf{r}) \equiv (\partial_x \rho_x - \partial_y \rho_y)/2$ and the striction $u_A(\mathbf{r}) \equiv (\partial_x \rho_x + \partial_y \rho_y)/2$ respectively, with $\rho_i(\mathbf{r})$ being the displacements along $i = (x, y)$ of the Fe atoms from their high temperature tetragonal equilibrium positions at \mathbf{r} .²⁰ The vectors $(\mathbf{q}', \mathbf{p}')$ are $\pi/2$ rotations of (\mathbf{q}, \mathbf{p}) respectively. Thus, $\lambda_O(q, p)$ and $\lambda_A(q, p)$ are the orthorhombic- and the striction- MECs. The $\mathbf{q} = \mathbf{p} = 0$ term, in particular, denotes the coupling of the static order parameters.

In this paper we calculate $\lambda_a(q, p)$ for $q, p \ll k_F$, $a = (O, A)$, from a microscopic model of fermions having nested Fermi pockets with typical Fermi wavevector k_F . The technical details are given in the Appendix A. Our main result is that, as the system approaches perfect nesting, $\lambda_a(q, p)$ diverges with a power-law. This implies

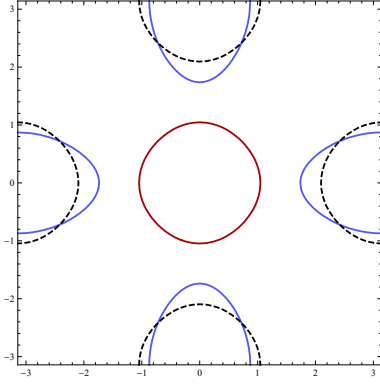


FIG. 1: (colour online) Fermi surface topology of the model without lattice distortions (see Eq. 2). Nesting between the hole pocket (solid, red) centered at $(0,0)$ and the electron pockets centered at $(\pi,0)$ and $(0,\pi)$ is tuned by the ellipticity η of the latter. Shown here are $\eta = 0.4$ (solid, blue) and the perfect nesting case with $\eta = 0$ (dashed, black).

that in nested metals the lattice deformations $u_a(\mathbf{q})$ are strongly coupled to certain *collective* electronic degrees of freedom. This coupling is to be contrasted with the standard electron-phonon case, where nesting induced phonon anomalies have weaker logarithmic singularity.²¹ We expect this result to be relevant for other metals that exhibit nesting induced density wave instabilities²² such as certain Cr based alloys,²³ organic conductors,²⁴ transition metal chalcogens such as NbSe₃,²⁵ and rare earth tellurides.²⁶ For FeAs systems this opens the possibility that $u_a(\mathbf{q})$ play a vital role in determining physical properties such as the superconducting gap structure.

For pedagogical reason we first calculate $\lambda_a(\mathbf{q} = \mathbf{p} = 0) \equiv \lambda_a$. For this we consider a three band model, defined by the Hamiltonian $\mathcal{H} = \mathcal{H}_0 + \mathcal{H}_I$ which has been used in the past for describing the FeAs systems.²⁷ The band dispersions are given by

$$\mathcal{H}_0 = \sum_{\mathbf{k},s} \left(\bar{\epsilon}_{\mathbf{k}}^{\alpha} \alpha_{\mathbf{k},s}^{\dagger} \alpha_{\mathbf{k},s} + \bar{\epsilon}_{\mathbf{k}}^{\beta} \beta_{\mathbf{k},s}^{\dagger} \beta_{\mathbf{k},s} + \bar{\epsilon}_{\mathbf{k}}^{\gamma} \gamma_{\mathbf{k},s}^{\dagger} \gamma_{\mathbf{k},s} \right), \quad (2)$$

where

$$\bar{\epsilon}_{\mathbf{k}}^n = \epsilon_0^n + 2(\bar{t}_x^n \cos k_x + \bar{t}_y^n \cos k_y)$$

with the band index $n = (\alpha, \beta, \gamma)$ and spin index s . We take

$$\begin{aligned} \bar{t}_x^n &= t_x^n (1 - p_x^n (u_O + u_A)), \\ \bar{t}_y^n &= t_y^n (1 + p_y^n (u_O - u_A)), \end{aligned}$$

such that $\bar{t}_{x/y}^n$ are the dispersions in the presence of uniform orthorhombic strain $u_O \equiv u_O(\mathbf{q} = 0)$ and striction $u_A \equiv u_A(\mathbf{q} = 0)$. We describe the hoppings in the absence of distortions by $t_{x/y}^{\alpha} = t = 1$ eV, $t_x^{\beta} = t_y^{\gamma} = t(1-\eta)$, $t_y^{\beta} = t_x^{\gamma} = -t(1+\eta)$, $\epsilon_0^{\beta} = \epsilon_0^{\gamma} = -\epsilon_0^{\alpha} = 3$ eV. Thus, the α -band describes a hole pocket centered at $(0,0)$ and the β -

and γ -bands describe electron pockets with ellipticity $\pm\eta$ and centered at \mathbf{Q}_1 and \mathbf{Q}_2 respectively. In the following we study how the MECs vary with η , with perfect nesting at $\eta = 0$ (see Fig. 1). For describing $\bar{t}_{x/y}^n$ we assume, following Su-Schrieffer-Heeger,^{28,29} that the changes in the hopping integrals are proportional to the strain-induced variations of the corresponding bond lengths. For details of the electron-lattice coupling see Appendix A 2. We expect that, in practice, the proportionality constants $p_{x/y}^n$ depend on the different orbital contents of the FeAs bands.³¹ Within the current simplified model we take $p_x^{\alpha} = p_x^{\beta} = p_1$, $p_y^{\beta} = p_x^{\gamma} = p_2$, $p_x^{\beta} = p_y^{\gamma} = p_3$ using C_4 symmetry, and we set $p_1 = p_2 = 2p_3 = 1$. Thus, the less dispersive directions at finite η are taken to be less sensitive to the distortions, thereby simulating the different orbital contents of the nested bands. Note that, the crucial ingredient here is the nesting η , while the other parameters enter the theory as quantitative details.

Next we define $\hat{\mathbf{m}}_{1,\mathbf{q}} = \alpha_{\mathbf{k},s_1}^{\dagger} \boldsymbol{\sigma}_{s_1 s_2} \beta_{\mathbf{k}+\mathbf{Q}_1+\mathbf{q},s_2}$ and $\hat{\mathbf{m}}_{2,\mathbf{q}} = \alpha_{\mathbf{k},s_1}^{\dagger} \boldsymbol{\sigma}_{s_1 s_2} \gamma_{\mathbf{k}+\mathbf{Q}_2+\mathbf{q},s_2}$, with $\boldsymbol{\sigma}$ denoting Pauli matrices and sum over repeated indices implied. We introduce the interaction

$$\mathcal{H}_I = -U \sum_{\mathbf{q}} (\hat{\mathbf{m}}_{1,\mathbf{q}}^{\dagger} \cdot \hat{\mathbf{m}}_{1,\mathbf{q}} + \hat{\mathbf{m}}_{2,\mathbf{q}}^{\dagger} \cdot \hat{\mathbf{m}}_{2,\mathbf{q}}). \quad (3)$$

We take $U = 0.07t$ to emphasize the weak coupling nature of the theory. In fact, the role of the interaction is merely to trigger a magnetic density wave transition within random phase approximation.

III. RESULTS

The derivation of λ_a , $a = (O, A)$ follows simply from thermodynamic considerations. The two terms of Eq. (3) are decoupled by introducing Hubbard-Stratanovich fields $(\mathbf{M}_{1,\mathbf{q}}^{\dagger}, \mathbf{M}_{1,\mathbf{q}})$ and $(\mathbf{M}_{2,\mathbf{q}}^{\dagger}, \mathbf{M}_{2,\mathbf{q}})$, respectively (see Appendix A 1).³⁰ Within random field approximation the critical magnetic free energy is $F_M = U(1 - U\chi_{m_1})(\mathbf{m}_1^2 + \mathbf{m}_2^2)$ (see Appendix A 4). Here $\mathbf{m}_1 = \langle \mathbf{M}_{1,0} \rangle$ and $\mathbf{m}_2 = \langle \mathbf{M}_{2,0} \rangle$ are the magnetic order parameters, and $\chi_{m_1} \equiv \chi(\mathbf{Q}_1, \omega = 0)$ is the bare static interband magnetic susceptibility at \mathbf{Q}_1 obtained from the Fourier transform of $\chi(\mathbf{Q}_1 + \mathbf{q}, \tau) = \langle T_{\tau} \mathbf{M}_{1,\mathbf{q}}^{\dagger}(\tau) \cdot \mathbf{M}_{1,\mathbf{q}}(0) \rangle / 3$, T_{τ} being the imaginary time ordering operator. Next, from the definition of the magnetoelastic free energy $F_{ME} \equiv \sum_a (\partial F_M / \partial u_a) u_a$,⁵ and comparing with Eq. 1, we get (see Appendix A 4)

$$\lambda_a = -U^2 (\partial \chi_{m_1} / \partial u_a)_{u_a=0}. \quad (4)$$

Since $\chi_{m_1} \propto \ln(\eta)$ due to the nesting, already from the above Eq. we expect that $\lambda_a \propto 1/\eta$ provided the distortions u_a change the *relative* ellipticity of the two bands. That this is indeed the case is evident from the expressions for $\bar{\epsilon}_{\mathbf{k}}^n$. Here we neglect strain dependence of U , since it gives non-singular contribution.

For simplicity we calculate λ_a at temperature $T = 0$ in the paramagnetic phase, and later comment about finite- T effects. In terms of the fermion dispersions we get

$$\lambda_a = 2U^2 \sum_{\mathbf{k}} \frac{\partial \bar{\epsilon}_{\mathbf{k}}^\alpha}{\partial u_a} \left[\frac{\delta(\epsilon_{\mathbf{k}}^\alpha)}{\epsilon_{\mathbf{k}+\mathbf{Q}_1}^\beta} - \frac{n_F(\epsilon_{\mathbf{k}}^\alpha) - n_F(\epsilon_{\mathbf{k}+\mathbf{Q}_1}^\beta)}{(\epsilon_{\mathbf{k}}^\alpha - \epsilon_{\mathbf{k}+\mathbf{Q}_1}^\beta)^2} \right] + \alpha \leftrightarrow \beta, \quad (5)$$

where $\epsilon_{\mathbf{k}}^n$ are the undistorted dispersions and n_F is the Fermi function. In the above the leading contribution is given by the terms with the δ -functions. To calculate the α -band Fermi surface contributions we note that, on this manifold $\epsilon_{\mathbf{k}+\mathbf{Q}_1}^\beta = 2t\eta(\cos k_x - \cos k_y)$ which has B_{1g} symmetry. The $(\cos k_x - \cos k_y)$ factor is precisely canceled by $(\partial \bar{\epsilon}_{\mathbf{k}}^\alpha / \partial u_a)$, the B_{1g} nature of which is guaranteed by the C_4 symmetry of the α -band. This gives rise to a singular $1/\eta$ contribution. Correspondingly, since $(\partial \bar{\epsilon}_{\mathbf{k}}^\alpha / \partial u_a)$ has A_{1g} symmetry, it does not contribute to the singularity of λ_A . On the other hand, as the β -band is only C_2 symmetric, $(\partial \bar{\epsilon}_{\mathbf{k}+\mathbf{Q}_1}^\beta / \partial u_a)$ have both B_{1g} and A_{1g} components, with the former giving singular contributions to both λ_O and λ_A . We finally get,

$$\lambda_a = -U^2 \nu_0 l_a / (\eta) + \dots, \quad (6)$$

where the ellipsis (here and henceforth) denote subleading terms, ν_0 is the density of states of the α -band at the Fermi surface, and $l_O = (2p_1 - p_2 - p_3)$ and $l_A = (p_2 - p_3)$. Experimentally, in all the FeAs systems λ_O is negative such that in the AF phase the ferromagnetic bonds are shorter than the antiferromagnetic ones. In this calculation we get the sign of the singular contribution to be negative by appropriately choosing $p_{x/y}$.

The fact that the remaining terms of Eq. 5 are subleading can be understood from the following argument. Near the crossing points of the two Fermi surfaces (which are potential sources of singularity) these terms can be expressed as $\text{Sgn}(\xi)/\xi^2$, where $\xi = \epsilon_{\mathbf{k}}^\alpha - \epsilon_{\mathbf{k}+\mathbf{Q}_1}^\beta$. This being odd, the power-law singularity cancels in the ξ -integral. If we take into account ξ -dependence of $(\partial \bar{\epsilon}_{\mathbf{k}}^\alpha / \partial u_a)$ etc, we obtain at most a subleading $\log \eta$ contribution. Finally, we verified the validity of Eq. 6 from a direct numerical evaluation of λ_a using Eq. 5, as demonstrated in Fig. 2.

In the above, the importance of the B_{1g} form factor stems from the fact that in the current model the perfect nesting is achieved by varying the ellipticity η . If, instead, we set $\eta = 0$ and tune the nesting between “circular” bands by varying $\theta = (|\epsilon_0^\alpha| - |\epsilon_0^\beta|)/|\epsilon_0^\alpha|$, we get singular $1/\theta$ terms that are associated with A_{1g} form factor. Thus, irrespective of how the nesting is tuned, the qualitative conclusion, namely the power-law divergence of λ_a remain unchanged. Note, though, that the FeAs bands are closer to a η -tuned nesting (at least at low doping), rather than a θ -tuned one where the two Fermi surfaces (after a \mathbf{Q}_1 shift of the β -band) do not cross each other.

Next, in order to calculate $\lambda_a(q, p)$, for $q, p \ll k_F$, we generalize the microscopic model of Eq. 2 to include the coupling between the electrons and the finite- q strains $u_a(\mathbf{q})$. This can be done conveniently in real

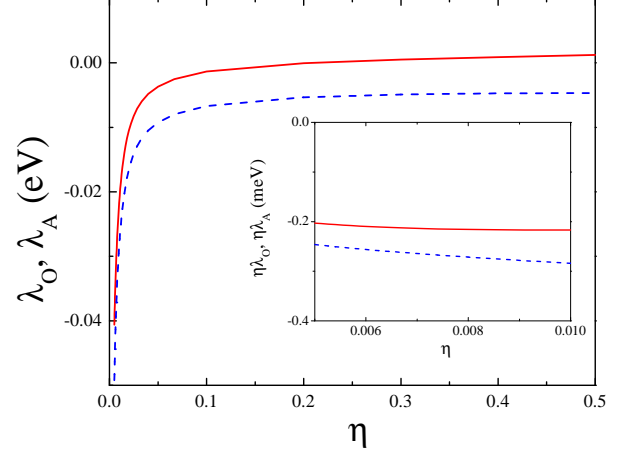


FIG. 2: (colour online) Divergence of the orthorhombic and the striction magnetoelastic constants (defined through Eq. 1) λ_O (solid, red) and λ_A (dashed, blue) as perfect nesting is approached by reducing the ellipticity η of the electron pockets. Inset shows saturation of $\eta\lambda_a$, $a = (O, A)$, at the lowest η , demonstrating the $1/\eta$ power-law (see Eq. 6).

space through the dependence of the hopping $\bar{t}_{x/y}^n$ to the relative atomic displacements $(\rho_{x/y}(\mathbf{r}) - \rho_{x/y}(\mathbf{r}'))$ between nearest neighbor sites \mathbf{r} and \mathbf{r}' (for details see Appendix A 2). After integrating out the electrons, and writing explicitly only the singular part of $\lambda_a(q, p)$ we get (see Appendix A 3)

$$\lambda_a(q, p) = 2U^2 \sum_{\mathbf{k}} \frac{\partial \bar{\epsilon}_{\mathbf{k}}^\alpha}{\partial u_a} \frac{n_F(\epsilon_{\mathbf{k}}^\alpha) - n_F(\epsilon_{\mathbf{k}-\mathbf{q}}^\alpha)}{(\epsilon_{\mathbf{k}}^\alpha - \epsilon_{\mathbf{k}-\mathbf{q}}^\alpha)(\epsilon_{\mathbf{k}}^\alpha - \epsilon_{\mathbf{k}+\mathbf{Q}_1+\mathbf{p}}^\beta)} + (\alpha \leftrightarrow \beta, \mathbf{p} \rightarrow -\mathbf{p}, \mathbf{q} \rightarrow -\mathbf{q}). \quad (7)$$

In the above the q - and p -dependencies are quite different. Since the q -dependent factors $(n_F(\epsilon_{\mathbf{k}}^n) - n_F(\epsilon_{\mathbf{k}+\mathbf{q}}^n))/(\epsilon_{\mathbf{k}}^n - \epsilon_{\mathbf{k}+\mathbf{q}}^n)$, with $n = (\alpha, \beta)$, are strongly peaked at $\epsilon_{\mathbf{k}}^n = 0$, it is justified to evaluate the remaining parts of the expression on the Fermi surfaces. For $p = 0$ we find that the q -dependence can be expressed by the Lindhard function $\chi_0(q)$ of the α -band. On the other hand, for $q \rightarrow 0$ and $p/k_F < \eta/2$, we find that the singularity and its pre-factor stays unchanged such that $\lambda_a(0, p) = \lambda_a(0, 0)$. In the opposite limit $p/k_F \gg \eta/2$, the $1/\eta$ singularity is absent. Taken together, Eq. 6 can be generalized to

$$\lambda_a(q, p) = -U^2 \chi_0(q) l_a / (\eta) + \dots, \quad (8)$$

for $p/k_F < \eta/2$ and $q/k_F \ll 1$. Thus, the coupling between the long wavelength modes involving the acoustic phonons and the collective spin fluctuations of the electrons has the same singularity as the coupling between the order parameters, and is therefore large, even if the bare electron-phonon coupling is weak.

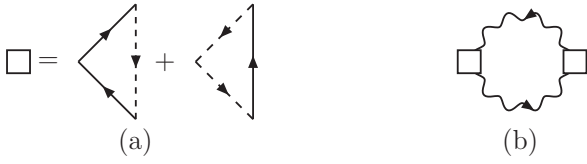


FIG. 3: (a) Diagrammatic representation of the magnetoelectric constants as the sum of fermionic triangles weighted by appropriate form factors (not shown). Solid and dashed lines imply holes and electrons respectively. (b) The fermionic triangles enter in the Azlamazov-Larkin graphs for certain correlation functions (see text), thereby providing nesting induced large contribution. The wavy lines imply antiferromagnetic spin fluctuations.

IV. DISCUSSION

In the following we comment on the implications of the above results for the FeAs systems, and more generally for nested metals.

(1) Since nesting is the only ingredient, we expect the results to be relevant for other nested metals. For e.g., in systems that show nesting induced charge density wave transitions,^{25,26} we expect large coupling between the long wavelength strains and the collective charge fluctuations.

(2) In the particular context of the FeAs, the relevance of the orthorhombic MEC $\lambda_O(q)$ has already been pointed out in several phenomenology-based studies.^{4-6,15} The current work bolsters these earlier studies by providing a means to understand why this coupling is large from a microscopic point of view. We note though, at least in the current simplified model, the singularities from the two nested bands have opposite signs, and therefore, for the pre-factor l_O to be non-zero it is crucial that their orbital contents be different, which is thought to be the case in FeAs.³¹ In practice, the pre-factors l_a in Eq. 8 need to be evaluated using *ab initio* tools, which is outside the scope of this work. Experimentally, the quantity λ_O can be obtained from a measurement of the variation of T_N with orthorhombic strain u_O .

(3) The relevance of the striction MEC $\lambda_A(q, p)$ is less obvious for the FeAs, even if it is large in the current model. Experimentally, T_N is more sensitive to uniaxial rather than hydrostatic pressure. One reason is that the striction elastic constant is large in contrast to the orthorhombic one which is known to be soft in the vicinity of the magneto-structural transitions. This effectively reduces the effect of hydrostatic pressure. A second possibility is that the coefficient l_A is small for the FeAs systems. In fact, instead of taking two electron bands as in the current model, if we consider nesting of the hole band with a single C_4 -symmetric electron band, we find $\lambda_A(q)$ to be non-singular because in this case $p_2 = p_3$.

(4) At finite T we get $\lambda_a(q, T) \propto 1/\max[T/|\epsilon_0^\alpha|, \eta]$, indicating a $1/T$ dependence at sufficiently large tem-

perature. The effect of finite lifetime is analogous.

(5) The above results also imply that nesting boosts spin fluctuation induced nematic softening. This is established most readily from the following argument using diagrams. The MECs can be represented by fermionic triangles with weight factors $(\partial \epsilon_{\mathbf{k}}^\alpha / \partial u_a)$ and $(\partial \epsilon_{\mathbf{k}+\mathbf{Q}_1}^\beta / \partial u_a)$ respectively (see Fig. 3(a) and Figs. 4, 5 of Appendix A). These triangles, in conjunction with the antiferromagnetic spin fluctuations around the ordering wavevectors $\mathbf{Q}_{1/2}$, also enter in the so-called Azlamazov-Larkin (AL) graphs for nematic susceptibilities whose vertices have B_{1g} symmetry (see Fig. 3(b)). The technical details are given in the Appendix B. Modeling the spin fluctuations by $D(\mathbf{q}, i\nu_n) = 1/(\delta + q^2 + |\nu_n|)$, where δ is the mass that vanishes at magnetic criticality, we get the AL contribution as

$$\chi_{AL} \sim (1/\eta)^2 \int'_{p, \nu_n} D(\mathbf{p}, i\nu_n)^2,$$

where the prime denote $\eta \gg q/k_F, \nu/t$. For $\delta \ll \eta^2$ we find that $\chi_{AL} \sim 1/\eta^2 \log(\eta^2/\delta)$. Thus, we conclude that in systems where the nesting is η -tuned, the AL contribution of the soft spin fluctuations will be enhanced by a factor $1/\eta^2$ for the static response functions of operators that are B_{1g} symmetric under point group transformations. This observation provides a rather general means to understand why spin fluctuations are effective in driving the various electronic spin-, charge-, and orbital-nematic softening,³²⁻³⁵ as well as the softening of the orthorhombic elastic constant.³⁶ Note that, while the importance of the AL contributions has been already emphasized,³⁷ the connection with nesting induced singularity has not been made earlier. Correspondingly, in systems where θ -tuned nesting is relevant, we expect softening of modes with A_{1g} symmetry.

(6) Finally, phenomenological studies have argued in favor of MEC also in the iron chalcogenide superconducting systems such as $\text{FeTe}_{1-x}\text{Se}_x$.^{6,38} However, just as the magnetic instability in these systems cannot be understood from a nesting point of view, similarly the current theory cannot be applied to argue in favor of large MEC in these materials. In other words, the MEC in the iron chalcogens is possibly a consequence of strong interaction and stems from the bond length dependence of the Heisenberg exchanges.

V. CONCLUSION

In the context of the iron arsenide materials, we studied the microscopic origin of the magnetoelastic couplings between the long wavelength in-plane strains of the lattice and the collective spin fluctuations of the electrons near the antiferromagnetic ordering wavevectors. Using a model of electrons with nested Fermi pockets, we find that these couplings diverge with a power-law as the system approaches perfect nesting. We expect this singularity to enter the susceptibilities of nematic variables via

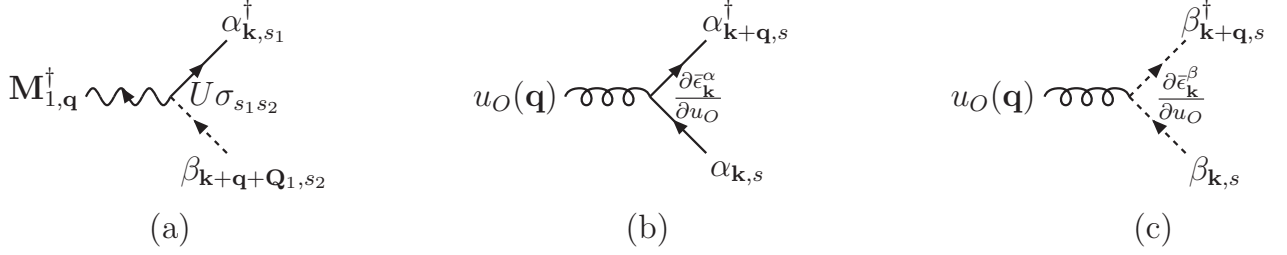


FIG. 4: (a) Interaction of spin fluctuations (wavy line) around $(\pi, 0)$ with fermions of the α -hole (solid line) and β -electron (dash line) bands. The interaction involving spin fluctuations around $(0, \pi)$ is similar (not shown). (b) & (c) Interaction of orthorhombic strain (gluon line) with fermions. The interaction involving striction is similar (not shown).

the Azlamasov-Larkin contributions. This implies nesting boosts spin fluctuation induced nematic softening. Moreover, in the future it will be interesting to study if, by means of the magnetoelastic couplings, the long wavelength strains affect the superconducting instability within a spin fluctuation mediated pairing scenario. Finally, our results are relevant for other materials that undergo density wave instabilities at nesting wavevectors.

Acknowledgments

The author is very thankful to P. M. R. Brydon, M. Civelli, Y. Gallais, P. Hirschfeld, C. Pépin, and C. Timm for insightful discussions.

Appendix A

In this section we provide a detailed derivation of the equations used in the main text starting from a microscopic model of interacting electrons which are also coupled to a square lattice. The system is described by the Hamiltonian

$$\mathcal{H} = \mathcal{H}_{\text{el}}^0 + \mathcal{H}_I + \mathcal{H}_{\text{el-lattice}}, \quad (\text{A1})$$

where the first two terms describe the electronic part, and the last term their coupling to the lattice distortions.

1. Electronic Hamiltonian

We use the three-bands model of Ref. 27, whose dispersions are described by

$$\mathcal{H}_{\text{el}}^0 = \sum_{\mathbf{k},s} \left(\epsilon_{\mathbf{k}}^\alpha \alpha_{\mathbf{k},s}^\dagger \alpha_{\mathbf{k},s} + \epsilon_{\mathbf{k}}^\beta \beta_{\mathbf{k},s}^\dagger \beta_{\mathbf{k},s} + \epsilon_{\mathbf{k}}^\gamma \gamma_{\mathbf{k},s}^\dagger \gamma_{\mathbf{k},s} \right), \quad (\text{A2})$$

where $\epsilon_{\mathbf{k}}^n = \epsilon_0^n + 2(t_x^n \cos k_x + t_y^n \cos k_y)$ with the band index $n = (\alpha, \beta, \gamma)$ and spin index s . We describe the

hoppings by $t_{x/y}^\alpha = t = 1$ eV, $t_x^\beta = t_y^\gamma = t(1 - \eta)$, $t_y^\beta = t_x^\gamma = -t(1 + \eta)$, $\epsilon_0^\beta = \epsilon_0^\gamma = -\epsilon_0^\alpha = 3$ eV. Thus, the α -band describes a hole pocket centered at $(0, 0)$ and the β - and γ - bands describe electron pockets with ellipticity $\pm\eta$ and centered at $\mathbf{Q}_1 = (\pi, 0)$ and $\mathbf{Q}_2 = (0, \pi)$ respectively. The associated Fermi surfaces are shown in Fig. 1 of the main text. The parameter η controls the nesting between the hole and the electron pockets, with $\eta = 0$ denoting the idealized situation of perfect nesting. Note that, in the absence of lattice distortions, \mathcal{H}_0 of Eq. (2) in the main text coincides with $\mathcal{H}_{\text{el}}^0$ defined above.

Next we define the interband spin operators

$$\begin{aligned} \hat{\mathbf{m}}_{1,q} &= \alpha_{\mathbf{k},s_1}^\dagger \boldsymbol{\sigma}_{s_1 s_2} \beta_{\mathbf{k}+\mathbf{Q}_1+\mathbf{q},s_2}, \\ \hat{\mathbf{m}}_{2,q} &= \alpha_{\mathbf{k},s_1}^\dagger \boldsymbol{\sigma}_{s_1 s_2} \gamma_{\mathbf{k}+\mathbf{Q}_2+\mathbf{q},s_2} \end{aligned}$$

with sum over repeated indices implied, and we introduce the interaction

$$\mathcal{H}_I = -U \sum_{\mathbf{q}} (\hat{\mathbf{m}}_{1,q}^\dagger \cdot \hat{\mathbf{m}}_{1,q} + \hat{\mathbf{m}}_{2,q}^\dagger \cdot \hat{\mathbf{m}}_{2,q}).$$

This is Eq. (3) in the main text. As noted there, the role of this interaction is only to trigger a spin density wave transition. We decouple the two interaction terms, which are quartic in fermion variables, by introducing the bosonic Hubbard-Stratanovich fields $(\mathbf{M}_{1,q}^\dagger, \mathbf{M}_{1,q})$ and $(\mathbf{M}_{2,q}^\dagger, \mathbf{M}_{2,q})$, respectively. After standard steps,³⁰ the interactions can be re-expressed as

$$\begin{aligned} \mathcal{H}_I &= U \sum_{\mathbf{q}} \left(\mathbf{M}_{1,q}^\dagger \cdot \mathbf{M}_{1,q} + \mathbf{M}_{2,q}^\dagger \cdot \mathbf{M}_{2,q} \right. \\ &\quad + \mathbf{M}_{1,q}^\dagger \cdot \alpha_{\mathbf{k},s_1}^\dagger \boldsymbol{\sigma}_{s_1 s_2} \beta_{\mathbf{k}+\mathbf{Q}_1+\mathbf{q},s_2} \\ &\quad \left. + \mathbf{M}_{2,q}^\dagger \cdot \alpha_{\mathbf{k},s_1}^\dagger \boldsymbol{\sigma}_{s_1 s_2} \gamma_{\mathbf{k}+\mathbf{Q}_2+\mathbf{q},s_2} + \text{h.c.} \right). \quad (\text{A3}) \end{aligned}$$

Formally, in the above, \mathcal{H}_I is quadratic in the fermion variables. The coupling between the bosonic Hubbard-Stratanovich fields and the fermions is shown graphically in Fig. 4 (a).

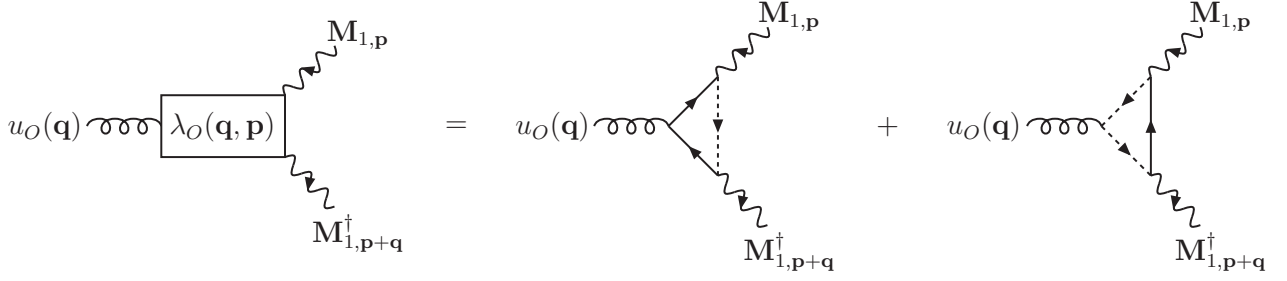


FIG. 5: Diagrammatic representation of the magnetoelastic coupling between the spin fluctuations (wavy line) around $(\pi, 0)$ and orthorhombic strain (gluon line). The couplings involving spin fluctuations around $(0, \pi)$ and striction are similar (not shown). The magnetoelastic couplings are three fermion excitations.

2. Electron-Lattice Coupling

We express the electron-lattice coupling as

$$\begin{aligned} \mathcal{H}_{\text{el-lattice}} = & - \sum_{\mathbf{r}, s} (\rho_x(\mathbf{r} + \hat{x}) - \rho_x(\mathbf{r})) \left(t_x^\alpha p_x^\alpha \alpha_{\mathbf{r}+\hat{x}, s}^\dagger \alpha_{\mathbf{r}, s} \right. \\ & + t_x^\beta p_x^\beta \beta_{\mathbf{r}+\hat{x}, s}^\dagger \beta_{\mathbf{r}, s} + t_x^\gamma p_x^\gamma \gamma_{\mathbf{r}+\hat{x}, s}^\dagger \gamma_{\mathbf{r}, s} + \text{h.c.} \Big) \\ & + x \rightarrow y. \end{aligned} \quad (\text{A4})$$

In the above $\rho(\mathbf{r})$ are the atomic displacements from their tetragonal equilibrium positions at \mathbf{r} . This is a two-dimensional and multiband generalization of the Su-Schrieffer-Heeger coupling introduced to study conducting polymers.^{28,29} Physically, it implies that the hoppings parameters depend on the bond-lengths, and that their variations are proportional to the variations in the bond-lengths. Here, (p_x^n, p_y^n) with $n = (\alpha, \beta, \gamma)$ are the band- and direction- dependent proportionality constants. They depend on the orbital contents of the bands, and, in practice, should be obtained using *ab initio* methods. In the current simplified model we take $p_x^\alpha = p_x^\beta = p_1$, $p_y^\beta = p_x^\gamma = p_2$, $p_x^\beta = p_y^\gamma = p_3$ using C_4 symmetry, and we set $p_1 = p_2 = 2p_3 = 1$. Next, we Fourier transform the above Eq. and we expand in small q since we are interested only in the coupling to the acoustic phonons and the uniform strains. Using the definition of the orthorhombic strain $u_O(\mathbf{r}) \equiv (\partial_x \rho_x - \partial_y \rho_y)/2$ and that of the striction $u_A(\mathbf{r}) \equiv (\partial_x \rho_x + \partial_y \rho_y)/2$, and their Fourier transforms $u_O(\mathbf{q}) = i(q_x \rho_x(\mathbf{q}) - q_y \rho_y(\mathbf{q}))/2$, and $u_A(\mathbf{q}) = i(q_x \rho_x(\mathbf{q}) + q_y \rho_y(\mathbf{q}))/2$, we get

$$\begin{aligned} \mathcal{H}_{\text{el-lattice}} = & -2 \sum_{\mathbf{q}, \mathbf{k}, s} [t_x^\alpha p_x^\alpha (u_O(\mathbf{q}) + u_A(\mathbf{q})) \cos k_x \\ & + t_y^\alpha p_y^\alpha (u_A(\mathbf{q}) - u_O(\mathbf{q})) \cos k_y] \alpha_{\mathbf{k}+\mathbf{q}, s}^\dagger \alpha_{\mathbf{k}, s} \\ & + (\alpha \rightarrow \beta) + (\alpha \rightarrow \gamma). \end{aligned} \quad (\text{A5})$$

In the limit $q \rightarrow 0$, where only the uniform orthorhombic and striction strains u_O and u_A are present, the hopping

parameters are modified compared to Eq. (A2) such that

$$\begin{aligned} t_x^n & \rightarrow \bar{t}_x^n = t_x^n (1 - p_x^n (u_O + u_A)), \\ t_y^n & \rightarrow \bar{t}_y^n = t_y^n (1 + p_y^n (u_O - u_A)). \end{aligned} \quad (\text{A6})$$

The corresponding dispersions $\bar{\epsilon}_{\mathbf{k}}^n$ in the presence of uniform strains, where

$$\bar{\epsilon}_{\mathbf{k}}^n = \epsilon_{\mathbf{k}}^n + 2(\bar{t}_x^n \cos k_x + \bar{t}_y^n \cos k_y), \quad (\text{A7})$$

are described in Eq. (2) of the main text. Using Eq. (A7) we can re-write Eq. (A5) as

$$\begin{aligned} \mathcal{H}_{\text{el-lattice}} = & \sum_{\mathbf{q}, \mathbf{k}, s} \left[\frac{\partial \bar{\epsilon}_{\mathbf{k}}^\alpha}{\partial u_O} u_O(\mathbf{q}) + \frac{\partial \bar{\epsilon}_{\mathbf{k}}^\alpha}{\partial u_A} u_A(\mathbf{q}) \right] \alpha_{\mathbf{k}+\mathbf{q}, s}^\dagger \alpha_{\mathbf{k}, s} \\ & + (\alpha \rightarrow \beta) + (\alpha \rightarrow \gamma). \end{aligned} \quad (\text{A8})$$

Examples of the above coupling is shown graphically in Fig. 4 (b) and (c).

3. Magnetoelastic Coupling

The magnetoelastic coupling is obtained by integrating out the fermions. This is possible because both the electron-electron interaction in Eq. (A3) and the electron-lattice interaction in Eq. (A8) are formally quadratic in the fermion variables. The result of this step is most readily understood in the diagrammatic language. Thus, the antiferromagnetic spin fluctuations (wavy lines) and the lattice distortions (gluon lines) are connected by internal fermion loops in Fig. 5. When the external frequencies are set to zero, the lowest order terms define an effective magnetoelastic Hamiltonian

$$\begin{aligned} \mathcal{H}_{ME} = & \sum_{\mathbf{q}, \mathbf{p}} \{ \lambda_O(q, p) u_O(\mathbf{q}) + \lambda_A(q, p) u_A(\mathbf{q}) \} \\ & \times \mathbf{M}_{1, \mathbf{q}+\mathbf{p}}^\dagger \cdot \mathbf{M}_{1, \mathbf{p}} + \dots, \end{aligned} \quad (\text{A9})$$

where the ellipses denote equivalent symmetry-related terms involving $(\mathbf{M}_{2, \mathbf{p}}^\dagger, \mathbf{M}_{2, \mathbf{p}})$. Note that, this is Eq. (1)

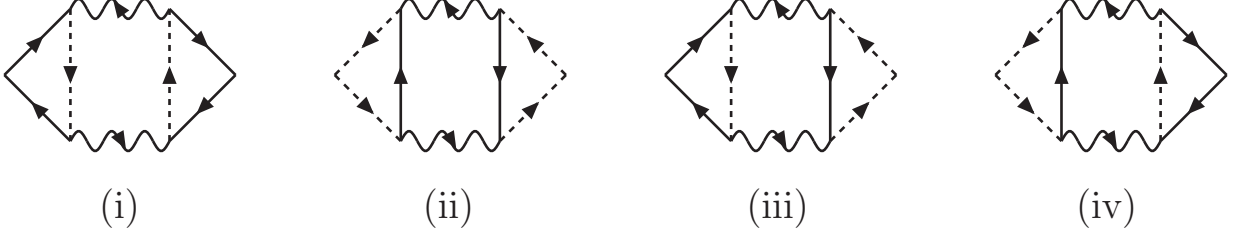


FIG. 6: Azlamasov-Larkin graphs representing contribution of spin fluctuations around $(\pi, 0)$ to the charge nematic susceptibility. There is similar contribution of the spin fluctuations around $(0, \pi)$ (not shown). The triangular vertices of the graphs, like the magnetoelastic couplings, are boosted by nesting.

in the main text. It is obvious from Fig. 5 that the magnetoelastic couplings $\lambda_a(q, p)$, with $a = (O, A)$, are nothing but convolutions of three fermion excitations. Thus,

$$\lambda_a(q, p) = \frac{2U^2}{\beta} \sum_{\mathbf{k}, \omega_n} \frac{\partial \bar{\epsilon}_{\mathbf{k}}^\alpha}{\partial u_a} G_\alpha(\mathbf{k}, i\omega_n) G_\alpha(\mathbf{k} - \mathbf{q}, i\omega_n) \times G_\beta(\mathbf{k} + \mathbf{p} + \mathbf{Q}_1, i\omega_n) + \{\alpha \leftrightarrow \beta, (\mathbf{p}, \mathbf{q}) \rightarrow (-\mathbf{p}, -\mathbf{q})\}. \quad (\text{A10})$$

Here β is inverse temperature, and the fermion Green's functions (in the absence of distortion) are given by $G_{\alpha/\beta}(\mathbf{k}, i\omega_n) = 1/(i\omega_n - \epsilon_{\mathbf{k}}^{\alpha/\beta})$. After the frequency summation, and keeping only the leading terms we get

$$\lambda_a(q, p) = 2U^2 \sum_{\mathbf{k}} \frac{\partial \bar{\epsilon}_{\mathbf{k}}^\alpha}{\partial u_a} \frac{n_F(\epsilon_{\mathbf{k}}^\alpha) - n_F(\epsilon_{\mathbf{k}-\mathbf{q}}^\alpha)}{(\epsilon_{\mathbf{k}}^\alpha - \epsilon_{\mathbf{k}-\mathbf{q}}^\alpha)(\epsilon_{\mathbf{k}}^\alpha - \epsilon_{\mathbf{k}+\mathbf{Q}_1+\mathbf{p}}^\beta)} + \{\alpha \leftrightarrow \beta, (\mathbf{p}, \mathbf{q}) \rightarrow (-\mathbf{p}, -\mathbf{q})\}, \quad (\text{A11})$$

which in the main text is Eq. 7. Setting the external momenta to zero, and at zero temperature we get

$$\lambda_a \equiv \lambda_a(\mathbf{q} = \mathbf{p} = 0) = 2U^2 \sum_{\mathbf{k}} \frac{\partial \bar{\epsilon}_{\mathbf{k}}^\alpha}{\partial u_a} \frac{\delta(\epsilon_{\mathbf{k}}^\alpha)}{\epsilon_{\mathbf{k}+\mathbf{Q}_1}^\beta} + \{\alpha \leftrightarrow \beta\}, \quad (\text{A12})$$

which are the leading terms (and the only ones of interest) in Eq. (5) of the main text. The evaluation of the r.h.s. of Eq. (A11) for small external momenta is described in the main text. This gives Eq. (8) of the main text, and, as a limiting case, Eq. (6) of the main text.

4. Derivation of λ_a from Thermodynamics

Note that, λ_a (i.e., with zero external momenta) defines the coupling between the order parameters of the magnetostructural transitions. Consequently, it is possible to obtain Eq. (A12) from thermodynamic arguments, without resorting to diagrams. This is the path followed in the main text. We repeat them here, for the sake of completeness, and also fill in with few details. After the Hubbard-Stratanovich transformation the critical part of

the magnetic free energy to one loop order (which is equivalent to random phase approximation) can be written as $F_M = U(1 - U\chi_{m_1})(\mathbf{m}_1^2 + \mathbf{m}_2^2)$. Here $\mathbf{m}_1 = \langle \mathbf{M}_{1,0} \rangle$ and $\mathbf{m}_2 = \langle \mathbf{M}_{2,0} \rangle$ are the magnetic order parameters, and $\chi_{m_1} \equiv \chi(\mathbf{Q}_1, \omega = 0)$ is the bare static interband magnetic susceptibility at \mathbf{Q}_1 obtained from the Fourier transform of $\chi(\mathbf{Q}_1 + \mathbf{q}, \tau) = \langle T_\tau \mathbf{M}_{1,\mathbf{q}}^\dagger(\tau) \cdot \mathbf{M}_{1,\mathbf{q}}(0) \rangle / 3$, T_τ being the imaginary time ordering operator. We get $\chi_{m_1} = 2 \sum_{\mathbf{k}} (n_F(\bar{\epsilon}_{\mathbf{k}}^\alpha) - n_F(\bar{\epsilon}_{\mathbf{k}+\mathbf{Q}_1}^\beta)) / (\bar{\epsilon}_{\mathbf{k}+\mathbf{Q}_1}^\beta - \bar{\epsilon}_{\mathbf{k}}^\alpha)$. Next, purely from symmetry argument, the magnetoelastic free energy can be written as

$$F_{ME} = \lambda_O u_O (\mathbf{m}_1^2 - \mathbf{m}_2^2) + \lambda_A u_A (\mathbf{m}_1^2 + \mathbf{m}_2^2). \quad (\text{A13})$$

Since F_{ME} is linear in the strains, it can be considered as a linear response of F_M in the presence of strains. This suggests that $F_{ME} \equiv \sum_a (\partial F_M / \partial u_a) u_a$, from which we get Eqs. (4) and (5) of the main text.

Appendix B

In this section we give further detail concerning the fifth point of the “discussion” which relates nematicity with magnetoelasticity. In particular, we show that, in complete analogy with magnetoelasticity, nesting of hole and electron pockets boosts critical spin fluctuation driven nematicity.

For the sake of concreteness we consider the charge nematic operator, which for the current model is given by

$$\hat{O} \equiv \sum_{\mathbf{k}, s} (\cos k_x - \cos k_y) (\alpha_{\mathbf{k}, s}^\dagger \alpha_{\mathbf{k}, s} + \beta_{\mathbf{k}, s}^\dagger \beta_{\mathbf{k}, s} + \gamma_{\mathbf{k}, s}^\dagger \gamma_{\mathbf{k}, s}).$$

We define the static nematic susceptibility as $\chi_n \equiv \int_0^\beta d\tau \langle \hat{O}(\tau) \hat{O}(0) \rangle$. In particular, we concentrate on the effect of critical spin fluctuations on χ_n . The relevant diagrams involving spin fluctuations ($\mathbf{M}_{1,\mathbf{q}}^\dagger, \mathbf{M}_{1,\mathbf{q}}$) and the α and β bands are shown in Fig. 6. Those involving ($\mathbf{M}_{2,\mathbf{q}}^\dagger, \mathbf{M}_{2,\mathbf{q}}$) and the α and γ bands give a factor 2 (not shown). These are the so-called Azlamasov-Larkin (AL) graphs. Writing the spin fluctuation propagator as

$D(\mathbf{q}, i\nu_n) = 1/(\delta + q^2 + |\nu_n|)$, where δ is the mass that vanishes at magnetic quantum criticality, we get the AL contribution

$$\chi_n^{AL} \propto \frac{1}{\beta} \sum_{\mathbf{p}, \nu_n} \Lambda(\mathbf{p}, i\nu_n, i\nu_n)^2 D(\mathbf{p}, i\nu_n)^2, \quad (\text{B1})$$

where

$$\begin{aligned} \Lambda(\mathbf{p}, i\nu_n, i\nu_n) = & \frac{1}{\beta} \sum_{\mathbf{k}, \omega_n} (\cos k_x - \cos k_y) G_\alpha(\mathbf{k}, i\omega_n)^2 \\ & \times G_\beta(\mathbf{k} + \mathbf{p} + \mathbf{Q}_1, i\omega_n + i\nu_n) \\ & + \{\alpha \leftrightarrow \beta, (\nu_n, \mathbf{q}) \rightarrow (-\nu_n, -\mathbf{q})\}. \quad (\text{B2}) \end{aligned}$$

On comparing Figs. 5 and 6, and Eqs. (A10) and (B2), it is clear that $\Lambda(\mathbf{p}, i\nu_n, i\nu_n)$, like the magnetoelastic couplings $\lambda_a(q, p)$, are convolutions of three-fermion excitations. Furthermore, noting that the $1/\eta$ singularity of $\lambda_a(q, p)$ is related to B_{1g} form factor, we conclude that for $(p/k_F, \nu_n/t) \ll \eta$, $\Lambda(\mathbf{p}, i\nu_n, i\nu_n) \propto 1/\eta$. In two space dimensions and for $\delta \ll \eta^2$ this eventually leads to the result quoted in the main text, namely $\chi_n^{AL} \sim 1/\eta^2 \log(\eta^2/\delta)$.

-
- ¹ Y. Kamihara, T. Watanabe, M. Hirano, and H. Hosono, J. Am. Chem. Soc. **130**, 3296 (2008).
 - ² For reviews see, e.g., M. Norman, Physics **1**, 21 (2008); D. C. Johnston, Adv. Phys. **59**, 803 (2010); G. R. Stewart, Rev. Mod. Phys. **83**, 1589 (2011); P. J. Hirschfeld, M. M. Korshunov, and I. I. Mazin, Rep. Prog. Phys. **74**, 124508 (2011); A. V. Chubokov, Annu. Rev. of Condens. Matter Phys. **3**, 57 (2012).
 - ³ I. I. Mazin and J. Schmalian, Physica C **469**, 614 (2009).
 - ⁴ R. M. Fernandes, L. H. VanBebber, S. Bhattacharya, P. Chandra, V. Keppens, D. Mandrus, M. A. McGuire, B. C. Sales, A. S. Sefat, and J. Schmalian, Phys. Rev. Lett. **105**, 157003 (2010).
 - ⁵ A. Cano, M. Civelli, I. Eremin, and I. Paul, Phys. Rev. B **82**, 020408(R) (2010).
 - ⁶ I. Paul, Phys. Rev. Lett. **107**, 047004 (2011).
 - ⁷ H.-H. Kuo, J. G. Analytis, J.-H. Chu, R. M. Fernandes, J. Schmalian, and I. R. Fisher, Phys. Rev. B **86**, 134507 (2012).
 - ⁸ R. M. Fernandes, A. E. Böhmer, C. Meingast, and J. Schmalian, Phys. Rev. Lett. **111**, 137001 (2013).
 - ⁹ D. J. Singh, and M. H. Du, Phys. Rev. Lett. **100**, 237003 (2008).
 - ¹⁰ I. I. Mazin, D.J. Singh, M. D. Johannes, and M. H. Du, Phys. Rev. Lett. **101**, 057003 (2008).
 - ¹¹ see, e.g., C. Liu, G. D. Samolyuk, Y. Lee, N. Ni, T. Kondo, A. F. Santander-Syro, S. L. Budko, J. L. McChesney, E. Rotenberg, T. Valla, A. V. Fedorov, P. C. Canfield, B. N. Harmon, and A. Kaminski, Phys. Rev. Lett. **101**, 177005 (2008); L. X. Yang, Y. Zhang, H. W. Ou, J. F. Zhao, D. W. Shen, B. Zhou, J. Wei, F. Chen, M. Xu, C. He, Y. Chen, Z. D. Wang, X. F. Wang, T. Wu, G. Wu, X. H. Chen, M. Arita, K. Shimada, M. Taniguchi, Z. Y. Lu, T. Xiang, and D. L. Feng, Phys. Rev. Lett. **102**, 107002 (2009); V. Brouet, M. Marsi, B. Mansart, A. Nicolaou, A. Taleb-Ibrahimi, P. Le Fèvre, F. Bertran, F. Rullier-Albenque, A. Forget, and D. Colson, Phys. Rev. B **80**, 165115 (2009).
 - ¹² see, e.g., C. Cao, P. J. Hirschfeld, and H.-P. Cheng, Phys. Rev. B **77**, 220506(R) (2008); J. Dong, H. J. Zhang, G. Xu, Z. Li, G. Li, W. Z. Hu, D. Wu, G. F. Chen, X. Dai, J. L. Luo, Z. Fang, and N. L. Wang, Europhys. Lett. **83**, 27006 (2008); V. Cvetkovic, Z. Tesanovic, Europhys. Lett. **85**, 37002 (2009); P. M. R. Brydon, J. Schmiedt, C. Timm, Phys. Rev. B **84**, 214510 (2011).
 - ¹³ L. Boeri, M. Calandra, I. I. Mazin, O. V. Dolgov, and F. Mauri, Phys. Rev. B **82**, 020506(R) (2010).
 - ¹⁴ C. Dhital, Z. Yamani, W. Tian, J. Zeretsky, A. S. Sefat, Z. Wang, R. J. Birgeneau, and S. D. Wilson, Phys. Rev. Lett. **108**, 087001 (2012).
 - ¹⁵ A. Cano and I. Paul, Phys. Rev. B **85**, 155133 (2012).
 - ¹⁶ J. Hu, C. Setty, and S. Kivelson, Phys. Rev. B **85**, 100507(R) (2012).
 - ¹⁷ J.-H. Chu *et al.*, J.-H. Chu, J. G. Analytis, K. De Greve, P. L. McMahon, Z. Islam, Y. Yamamoto, I. R. Fisher, Science **329**, 824 (2010); M. A. Tanatar *et al.*, M. A. Tanatar, E. C. Blomberg, A. Kreyssig, M. G. Kim, N. Ni, A. Thaler, S. L. Budko, P. C. Canfield, A. I. Goldman, I. I. Mazin, and R. Prozorov, Phys. Rev. B **81**, 184508 (2010); H.-H. Kuo, J.-H. Chu, S. C. Riggs, L. Yu, P. L. McMahon, K. De Greve, Y. Yamamoto, J. G. Analytis, and I. R. Fisher, Phys. Rev. B **84**, 054540 (2011); T. Liang, M. Nakajima, K. Kihou, Y. Tomioka, T. Ito, C. H. Lee, H. Kito, A. Iyo, H. Eisaki, T. Kakeshita, and S. Uchida, J. Phys. Chem. Solids **72**, 418 (2011).
 - ¹⁸ M. G. Kim, R. M. Fernandes, A. Kreyssig, J. W. Kim, A. Thaler, S. L. Budko, P. C. Canfield, R. J. McQueeney, J. Schmalian, and A. I. Goldman, Phys. Rev. B **83**, 134522 (2011); C. R. Rotundu and R. J. Birgeneau, Phys. Rev. B **84**, 092501 (2011).
 - ¹⁹ M. Tomic, H. O. Jeschke, R. M. Fernandes, R. Valenti, Phys. Rev. B **87**, 174503 (2013).
 - ²⁰ see, e.g., L. D. Landau and E. M. Lifshitz, *Theory of Elasticity*, Sec. 10 (Pergamon Press, Oxford, 1970).
 - ²¹ G. L. Zhao and B. N. Harmon, Phys. Rev. B **45**, 2818 (1992).
 - ²² R. E. Peierls, *Quantum Theory of Solids* (Clarendon, Oxford, 1964).
 - ²³ see, e.g., E. Fawcett, Rev. Mod. Phys. **60**, 209 (1988); A. Yeh, Y.-A. Soh, J. Brooke, G. Aeppli, T. F. Rosenbaum, S. M. Hayden, Nature **419**, 459 (2002).
 - ²⁴ see, e.g., D. Jérôme and H. Schulz, Adv. Phys. **31**, 299 (1982).
 - ²⁵ see, e.g., J. Schäfer, E. Rotenberg, S. D. Kevan, P. Blaha, R. Claessen, and R. E. Thorne, Phys. Rev. Lett. **87**, 196403 (2001); P. Moceau, Adv. Phys. **61**, 325 (2012).
 - ²⁶ see, e.g., E. DiMasi, B. Foran, M. C. Aronson, and S. Lee, Phys. Rev. B **54**, 13587 (1996); V. Brouet, W. L. Yang, X.

- J. Zhou, Z. Hussain, N. Ru, K. Y. Shin, I. R. Fisher, and Z. X. Shen, Phys. Rev. Lett. **93**, 126405 (2004); J. Laverock, S. B. Dugdale, Zs. Major, M. A. Alam, N. Ru, I. R. Fisher, G. Santi, and E. Bruno, Phys. Rev. B **71**, 085114 (2005);
- ²⁷ J. Knolle, I. Eremin, A.V. Chubukov, and R. Moessner, Phys. Rev. B **81**, 140506(R) (2010).
- ²⁸ W. P. Su, J. R. Schrieffer, and A. J. Heeger, Phys. Rev. Lett. **42**, 1698 (1979).
- ²⁹ A. J. Heeger, S. Kivelson, J. R. Schrieffer, W. P. Su, Rev. Mod. Phys. **60**, 781 (1988).
- ³⁰ see, e.g., A. Auerbach, *Interacting Electrons and Quantum Magnetism*, Chapter 16.5 (Springer-Verlag, New York, 1994).
- ³¹ see, e.g., K. Kuroki, S. Onari, R. Arita, H. Usui, Y. Tanaka, H. Kontani, and H. Aoki, Phys. Rev. Lett. **101**, 087004 (2008); S. Graser, T. A. Maier, P. J. Hirschfeld, and D. J. Scalapino, New J. Phys. **11**, 025016 (2009); M. Daghofer, A. Nicholson, A. Moreo, E. Dagotto, Phys. Rev. B **81**, 014511 (2010); P. M. R. Brydon, M. Daghofer, and C. Timm, J. Phys.: Condens. Matter **23**, 246001 (2011).
- ³² see, e.g., R. M. Fernandes and J. Schmalian, Supercond. Sci. Technol. **25**, 084005 (2012).
- ³³ Y. Gallais, R. M. Fernandes, I. Paul, L. Chauviere, Y.-X. Yang, M.-A. Measson, M. Cazayous, A. Sacuto, D. Colson, and A. Forget, Phys. Rev. Lett. **111**, 267001 (2013); H. Yamase and R. Zeyher, Phys. Rev. B **88**, 180502(R) (2013).
- ³⁴ see e.g., Y. K. Kim, W. S. Jung, G. R. Han, K.-Y. Choi, C.-C. Chen, T. P. Devereaux, A. Chainani, J. Miyawaki, Y. Takata, Y. Tanaka, M. Oura, S. Shin, A. P. Singh, H. G. Lee, J.-Y. Kim, and C. Kim, Phys. Rev. Lett. **111**, 217001 (2013);
- ³⁵ J.-H. Chu, H.-H. Kuo, J. G. Analytis, and I. R. Fisher Science **337**, 710 (2012).
- ³⁶ M. Yoshizawa, D. Kimura, T. Chiba, A. Ismayil, Y. Nakanishi, K. Kihou, C.-H. Lee, A. Iyo, H. Eisaki, M. Nakajima, S. Uchida, J. Phys. Soc. Jpn. **81** 024604 (2012); A. E. Böhmer, P. Burger, F. Hardy, T. Wolf, P. Schweiss, R. Fromknecht, M. Reinecker, W. Schranz, C. Meingast, Phys. Rev. Lett. **112**, 047001 (2014).
- ³⁷ S. Onari, H. Kontani, Phys. Rev. Lett. **109**, 137001 (2012); H. Kontani and Y. Yamakawa, Phys. Rev. Lett. **113**, 047001 (2014).
- ³⁸ I. Paul, A. Cano, and K. Sengupta, Phys. Rev. B **83**, 115109 (2011).